

**MODELLING THE RELEASE OF VOLATILE FISSION PRODUCT CESIUM FROM
CANDU FUEL UNDER SEVERE ACCIDENT CONDITIONS
USING ARTIFICIAL NEURAL NETWORKS**

W.S. ANDREWS and B.J. LEWIS

Department of Chemistry and Chemical Engineering
Royal Military College of Canada
Kingston, Ontario K7K 7B4



CA0000069

D.S. COX

Atomic Energy of Canada Limited Research Company
Chalk River Laboratories
Chalk River, Ontario K0J 1J0

ABSTRACT

An artificial neural network (ANN) model has been developed to predict the release of volatile fission products from CANDU fuel under severe accident conditions. The model was based on data for the release of ^{134}Cs measured during three annealing experiments (Hot Cell Experiments 1 and 2, or HCE-1, HCE-2 and Metallurgical Cell Experiment 1, or MCE-1) at Chalk River Laboratories. These experiments were comprised of a total of 30 separate tests. The ANN established a correlation among 14 separate input variables and predicted the cumulative fractional release for a set of 386 data points drawn from 29 tests to a normalized error, E_n , of 0.104 and an average absolute error, E_{abs} , of 0.064. Predictions for a blind validation set (test HCE2-CM6) had an E_n of 0.064 and an E_{abs} of 0.054. A methodology is presented for deploying the ANN model by providing the connection weights. Finally, the performance of an ANN model was compared to a fuel oxidation model developed by Lewis et al. and to the U.S. Nuclear Regulatory Commission's CORSOR-M.

INTRODUCTION

The need to define nuclear power reactor source terms for fission products released during severe accident conditions has been underscored by the accidents at Three Mile Island and Chernobyl. In the United States, tests have been conducted involving the heating, or annealing, of fuel fragments and short segments of Light Water Reactor (LWR) fuel rods under varying environmental conditions, such as steam and hydrogen.¹ Analysis of early annealing experiments performed at the Oak Ridge National Laboratory (ORNL) has provided a correlation of the cumulative release of volatile fission products with temperature and time in a steam environment. This correlation, called CORSOR-M, is used by the United States Nuclear Regulatory Commission for LWR source term prediction.² Its applicability to CANDU pressurized heavy water reactor (PHWR) fuel has yet to be established. Further, it only considers two variables (temperature and time) in one environment (steam).

Corresponding annealing experiments have been conducted at the Chalk River Laboratories (CRL) on fuel fragments and mini-elements of CANDU fuel. In fact, the Hot Cell Experiments 1 and 2 (HCE-1 and HCE-2)^{3,4} and the Metallurgical Cell Experiment (MCE-1)⁵ include a total of 30 separate tests conducted under a wide variety of sample sizes, conditions and environments. The resulting large data base has yet to be analyzed to the point that an overall comprehensive model could predict experimental results with any degree of confidence.

The physical mechanisms involved in the release of volatile fission products under severe accident conditions are felt to be extremely complex. In the U.S., the FASTGRASS code has been developed to model such phenomena as fission gas bubble nucleation, migration, interlinking and resolution,⁶ while in Canada, SOURCE-2 is a mechanistic model for CANDU fuel.⁷ Both of these codes, however, are computationally intensive and thus do not run in real time. As a result, work continues on simpler, semi-empirical models which are based on the controlling physical phenomena. Examples of this are recent work by Osborne and Lorenz at ORNL⁸ and by Lewis et al. in Canada.⁹ This notwithstanding, the comprehensive model of fission product release considering the full spectrum of conditions of the annealing tests and able to run in real time has not appeared yet. This paper will outline a novel approach to empirically modelling the results of 29 CRL tests with the use of an artificial neural network (ANN) in order to predict the cumulative fission product release of volatile fission products (specifically ¹³⁴Cs).

ARTIFICIAL NEURAL NETWORKS

Neural network development began in the mid 1940's, but went into a hiatus due to a lack of discernible applications and sufficiently powerful computers. The most widely-used paradigm, back propagation, emerged in the mid 1980's from the work of two psychologists, McClelland and Rumelhart, in their efforts to model the functioning of the brain.¹⁰ Neural networks are composed of simple nodes (neurons) which take inputs, sum them, perform a simple mathematical operation on this sum via a transfer function and pass the result on to other nodes. Before the output arrives at a subsequent node, however, a weight is applied to it. As a consequence, nodes receive outputs of preceding nodes which have been modified by these weights.

Current practice in back propagation networks is to use three layers of neurons, with interconnections as shown in Figure 1. (Recent usage also exhibits some degree of connection directly between the input and output nodes, in addition to the connections indicated in Figure 1.) These layers are usually named input (X), hidden (Y) and output (Z). The input layer contains the values of the variables and parameters considered for correlation. In this application, each node would correspond to a value from the list in Table 1. These inputs are mapped into the range -1.0 to +1.0 using the mapping function

$$x_i = \frac{2v_i - (M_i + m_i)}{(M_i - m_i)}, \quad (1)$$

where x_i is the scaled or mapped i^{th} input value, corresponding to v_i , the unscaled or raw input value. M_i and m_i are the maximum and minimum values of v_i , respectively. Each input node is connected to each node in the hidden layer. It is also usual to connect a bias node (with a set value of unity [1]) to all hidden and output nodes. The bias node serves to offset the origin of the

transfer function and tends to cause the network to converge more quickly.

Each connection to a hidden layer node contains the normalized input value leaving the input layer or bias node, modified by a connection weight. Thus, the i^{th} scaled input value, x_i , connected to the j^{th} hidden node has a weight, w_{ji} , applied to it. Consequently, the hidden node receives as an input from the i^{th} node, the value $w_{ji}x_i$. Also, as noted above, each node receiving inputs sums these inputs. In Figure 2, I_j is the sum of i inputs, each multiplied by its own connection weight, so that

$$I_j = \sum_{i=0}^n w_{ji} x_i. \quad (2)$$

When optimized, this is the equation of a linear regression, with the intercept being the weight associated with the bias node, w_{j0} .

Non-linearity is introduced into the model by the transfer function, which is applied to the summed inputs, I_j . Several different functions are available (sinusoidal, sigmoidal), but the one most widely used is the hyperbolic tangent, which is the smooth version of the step function from -1 to +1. The application of the tanh transfer function yields an output, y_j , from the j^{th} hidden node, such that

$$y_j = \frac{e^{I_j} - e^{-I_j}}{e^{I_j} + e^{-I_j}} = \tanh I_j. \quad (3)$$

This same process is repeated between the hidden layer and the output layer, with the transfer function again applied to the summed inputs to produce the output. Thus

$$I_k = \sum_j w_{kj} y_j, \quad (4)$$

where I_k is the sum of the weighted inputs to the k^{th} output node and w_{kj} is the connecting weight between the k^{th} output node and the j^{th} hidden node (or the bias node). The scaled output from the k^{th} output node is given by

$$z = \tanh I_k. \quad (5)$$

This output value z must then be mapped back to provide a real value for the cumulative fractional release f . This process is similar to but the reverse of the input mapping. Thus

$$f = \frac{(M - m)z + (Rm - rM)}{R - r}, \quad (6)$$

where M and m are the measured maximum and minimum values of the output variable f and R and r are the maximum and minimum values of the network output z (here 0.8 and -0.8 respectively).

When the network is initialized, the values of the weights are randomly assigned. The "knowledge" or "artificial intelligence" within the network, however, resides in the distribution of these weights which must be adjusted to be able to produce an output as close as possible to the desired output. This process of adjusting the weights is called supervised learning and is conducted during the training phase of the network development.

To effect training, the network is not only presented with a full array of inputs, but also with known (measured) outputs for each input set. When the initial pass through the network for a given set of data is complete, an output, z , is determined. This value is then compared to the desired output value, d (the scaled measured value of the cumulative fractional release), to arrive at a global error E :

$$E = 0.5(d - z)^2, \quad (7)$$

The global error is then propagated backwards through the network to adjust the individual connecting weights. This back and forth iterative process is continued until the global error is minimized. At this point, another set of input data (vector) is introduced into the network and the process is repeated. Generally, the connecting weights are adjusted after an "epoch" of up to about 500 different inputs (this can be adjusted to facilitate learning, but updates are rarely done after each input set, in order to prevent oscillations in weight values).

Once training is complete, the network is tested against data which had not been seen during training. Like the training set, the test set should represent, to the greatest extent possible, the whole range of the input space. Also, like the training set, the test set must have known output values available for comparison with the network predicted values. Finally, the network should be validated by predicting results for a data set representative of a likely application.

Essentially, then, a trained neural network is an n -dimensional correlation, and provides a result similar to a non-linear regression. The link with the physical phenomena it is modelling is through the choice of variables or parameters. Any relationship among these inputs is established by the learning rule itself, and not by any real or postulated physical relationships.

Neural networks have a number of advantages over other types of models or correlations:

1. With the "knowledge" or "intelligence" distributed throughout the network, a reasonable response is possible when the input space contains incomplete, noisy or previously unseen values.
2. A careful analysis of the weights throughout the network permits the various parameters or variables in the input space to be ranked in order of influence on the output.
3. A trained neural network model operates in real time, making it suitable for being embedded in much more complex computer codes, such as modelling the progression of a severe reactor accident.

EXPERIMENTAL

The data base used to construct the model comprised 9 tests of HCE-1, 12 of HCE-2 and 8 of MCE-1, with the tests conducted between 1350 and 2100°C and in steam, air or argon/hydrogen atmospheres. Each annealing test involved placing a fragment or mini-element in an induction furnace, and introducing the appropriate environment (steam, air or argon/hydrogen) into the furnace. The release of fission products from the sample was determined by measuring the change in fission product activity by using gamma ray spectrometry. As well as environment, other factors varied included temperature, time at temperature, heating ramp rate, sample size, amount of zircaloy cladding and sample burnup. The fission products measured included ^{134}Cs and ^{137}Cs , ^{103}Ru and ^{131}I , although the model reported on in this paper was developed for ^{134}Cs , as the cumulative release values showed minimal randomness and the cesium behaviour was felt to be representative of volatile fission products in general.

ANALYSIS

The neural net used to model the CRL tests was based on *NeuralWorks Professional II/Plus* by NeuralWare¹¹ and featured 14 different inputs, as listed in Table 1. Related to Figure 1, the input space would extend from x_1 to x_{14} . A single hidden layer was used with differing numbers of nodes (from 2 to 15). All the architectures returned comparable results, except the networks with only 2 hidden nodes, which provided poor correlations. The output layer contained a single node and represented the cumulative fractional release of ^{134}Cs .

Much of the effort needed to train a neural network must be invested in creating the data base to provide the input vectors. Each test contained values for temperature and cumulative fractional release measured at intervals of 100 to 300 s. Most tests exhibited a characteristic response of an initial plateau on the Time/Fractional Release curve (Figure 3) displaying an initial low release rate (typically as a result of non-oxidizing conditions), a fairly steep climb due to an increased release rate from diffusion and grain boundary release (particularly during oxidizing conditions and a final plateau, indicating some trapping in the fuel porosity. Most of the data provided, then, were confined to the initial and final plateaus, with little available from the high release rate portion. Further, more tests were conducted at 1600°C than at any other temperature, although the isothermal test temperatures ranged from 1350 to 2100°C. In order for the model to be able to interpolate with any degree of confidence, the input space had to be as balanced as possible. Without this, inadvertent biases would be introduced and trained into the network. In other words, the network would tend to provide better predictions for conditions approximating the preponderance of training data and provide poorer predictions for other areas in the input space. To redress this imbalance, the data available for each test were expanded significantly by interpolation, so that the available number of training vectors was increased from 1371 to 4049. Any inaccuracies introduced by this approach were felt to be well within the actual noise of the data itself.

The expanded data base was separated into two portions, with 90% of the data provided for the training set and the remaining 10% for the test set. In order to achieve balance, data from some tests were repeated, so that the total input space contained 12,516 vectors. Further, the results from a complete test, HCE2-CM6, were withheld from both the above sets to provide a validation by exposing the trained network to conditions it had not been trained on.

Model effectiveness was gauged in three ways:

1. Network predicted cumulative fractional releases (outputs) were plotted against the corresponding values actually determined by CRL. A perfect correlation would have all points fall along the diagonal with a slope of 1 and an intercept of 0. The corresponding values from the linear regression through the data were then computed, including the slope and the correlation coefficient, r , which is the covariance divided by the product of the sample standard deviations.¹²
2. The normalized error, E_n , is the ratio of the average sum-squared error to the average of the squared deviations. This value is felt to be particularly useful for back propagation, as networks learn the average or smoothed target values. The normalized error, then, can be considered as reflecting the proportion of the output variance that is due to error, rather than the network architecture itself.
3. The average absolute error, E_{abs} , is the average difference (in absolute terms) between the measured and predicted values for a test or validation set.

As noted already, networks of differing numbers of hidden nodes had comparable r values for the test set. An example of the scatter plot for a network having 5 hidden nodes in one hidden layer can be seen in Figure 4. The solid dots show a perfect correlation, which can be compared with the actual linear regression through the points. Most of the 386 test vectors provide points very close or on the regression lines. Overall, the slope of .899 and intercept of .080 are fairly close to the optimal values of 1 and 0 respectively. The r value of .946 shows that the regression itself accounts for 94.6% of the dispersion in the data, with the remainder attributable to the data itself.

The validation of the network involved using the vectors of a complete test, HCE2-CM6, with the results contained in Figure 5. For this particular test, the network provides a good linear correlation (r is very good at .99), although it slightly underpredicts in the steam portion of the test and overpredicts in the inert portion. As shown in Table 2, the E_n value is 0.064, while E_{abs} is 0.054 over the whole test. Returning to Figure 4, however, it can be seen that some tests are underpredicted while others are overpredicted, while the vast majority of vectors are well predicted.

Figure 6 shows the measured and predicted cumulative fractional releases plotted against time that the sample is above 1000°C. Two points are of note here. The neural network model provides a smoothing of the data, with the exception of the discontinuity at about 4000 s (the point at which the environment changed from inert to steam). The second point is that the model is able to reproduce the non-linearity of the relationship between fractional release and time, due to varying release rates. In this particular test, though, the model values diverge from the measured at less than 4000 s and beyond about 7500 s.

A sensitivity analysis and an examination of the distribution of connection weights was conducted (the most significant inputs should have the highest connecting weights). The results can be seen in Table 3. The fuel temperature was found to be the predominant influence in predicting the cumulative fractional release of ¹³⁴Cs, while time was second to temperature but

more important than all other factors. The weight of Zircaloy followed time and reflected the presence or absence of a physical barrier (cladding) as well as its chemical influence (due to hydrogen production from metal-water reactions), which affect the fuel oxidation kinetics as a result of a lower oxidation potential. The hierarchy of the remaining influences is felt to be somewhat ambiguous, with these variables being second order influences, at best. The relatively minor role of closed cladding may also suggest that the cladding on the fuel samples was never really closed, as the end caps were only held loosely by wires. This, plus evidence of double sided oxidation¹³ indicates that the cladding may never have provided a significant physical barrier to the release of cesium. The relative importance of time suggests that much of the inventory was intragranular, with diffusion to the grain boundary surface and interconnected pore network. Further, the relatively modest influence of the fuel weight (varying over two orders of magnitude), and thus the surface-to-weight ratio, reinforces the significance of the intragranular inventory.

In addition, there was relatively little range of values in the linear power and burnup of the fuel samples. Not surprisingly, then, these variables had relatively little influence on the cumulative fractional release of cesium from the range of test samples.

Finally, the ANN model was compared to CORSOR-M and to the Lewis et al. fission product release model.⁹ The results can be seen graphically in Figures 5 and 6 applied to the same validation set used in the ANN development, HCE2-CM6. The models are compared statistically in Table 2. It can be seen that the CORSOR-M model greatly underestimated the release fraction. This may be attributable to the different experimental conditions upon which CORSOR-M was developed, i.e., higher temperatures and larger fuel samples. The performance of the Lewis model is quite good, although it must be borne in mind that the model is fixed at the experimentally measured release fraction at the introduction of steam. In contrast, the ANN model is a pure or blind prediction of the HCE2-CM6 measured releases in both inert and steam environments. It should be noted, however, that the model depicted in Figures 5 and 6 is not the same as the one in Figure 4. Both models were trained from the same data set and had comparable architectures, but one (shown in Figure 4) provided the best overall predictions of all the ANN models developed across the whole set of 29 tests. The other ANN model, shown in Figures 5 and 6, provided a better prediction for the specific validation set chosen, HCE2-CM6. Of the two models, it is felt the one with the better general behaviour (Figure 4) is the more useful, so this was the one chosen for deployment.

The overall relative closeness of the ANN model predictions to the values measured by CRL indicates that a trained neural network model has been able to establish a good correlation between a number of disparate parameters representative of possible severe reactor accident conditions and the cumulative fractional release of fission product cesium. A similar ANN model was developed to predict the release of volatile fission products from LWR fuel based on the VI series of experiments at Oak Ridge National Laboratory.¹⁴ A more full explanation of ANN models developed for the release of fission products from both CANDU and LWR fuel is available.¹⁵

ANN MODEL DEPLOYMENT

The ANN models were developed from an input space of 14 variables, as shown in Table 1. In order to use a trained model to predict the cumulative fractional release of cesium under

conditions within the range of input values, the appropriate variable values must be scaled according to Eq. (1). The appropriate maximum and minimum values are contained in Table 1. The connection weights for the 14-5-1 (bias node 0, input nodes 1-14, hidden nodes 15-19 and output node 20) network shown in Figure 4 are contained in Table 4. The output values from each input node must then be multiplied by the appropriate connection weight and summed at each hidden node (Eq. (2)). A hyperbolic tangent transfer function is then applied at each hidden node to determine the appropriate output (Eq. (3)). This process is repeated at the output node (Eqs. (5) and (6)). The output from the output node must then be scaled back to a real world value, according to Eq. (7), with the respective values of M and m being 1.023 and 0. This series of operations can easily be performed by a spreadsheet calculation or written into a short code in a programming language, e.g., Basic. The series of simple calculations allows the computations to be performed in real time.

CONCLUSIONS

A back propagation neural network model with a modified delta learning rule has been trained to predict the cumulative fractional release of the volatile fission product cesium from CANDU fuel fragments and mini-elements under a variety of simulated severe accident conditions. The model was able to reproduce the non-linearities inherent in the relationship between fractional release and time, and provided a smoothing of the data. Finally, the model was able to predict the general trend of the release kinetics for a validation set which was not used for training, and to predict the cumulative fractional release to within an average absolute error of 0.054.

ACKNOWLEDGEMENTS

The authors gratefully acknowledge the use of the experimental data performed by the Fission Product Release Group of the Fuel Engineering Branch at the Chalk River Laboratories. The experimental work was funded by Atomic Energy of Canada Limited, Ontario Hydro, Hydro Quebec, and New Brunswick Electric Power Corporation under the CANDU Owners Group agreement. The work performed at the Royal Military College was funded by the Academic Research Program of the Department of National Defence of Canada under allocation 3705-882.

REFERENCES

1. OSBORNE, M.F. and LORENZ, R.A., "Results of ORNL VI Series Fission Product Release Tests", Proceedings of the 20th Water Reactor Safety Information Meeting, Bethesda, Maryland, 21-23 Oct (1992).
2. KUHLMAN, M.R., LEHMICKE, D.J. and MEYER, R.O., "CORSOR User's Manual", NUREG/CR- 4173, USNRC Mar (1985).
3. COX, D.S., LIU, Z., ELDER, P.H., HUNT, C.E.L. and ARIMESCU, V.I., "Fission-Product Release Kinetics from CANDU and LWR Fuel During High-Temperature Steam Oxidation Experiments", presented at the IAEA Technical Meeting on Fission Gas Release and Fuel Rod Chemistry Related to Extended Burnup, Pembroke, Ontario, 28 Apr to 1 May (1992).

4. COX, D.S., LIU, Z., DICKSON, R.S. and ELDER, P.H., "Fission-Product Releases During Post-Irradiation Annealing of High Burnup CANDU Fuel", presented at the Third International Conference on CANDU Fuel, Pembroke, Ontario, 4-8 Oct (1992).
5. LEWIS, B.J., IGLESIAS, F.C., HUNT, C.E.L. and COX, D.S., "Release Kinetics of Volatile Fission Products Under Severe Accident Conditions", Nucl. Technol., **99**, 330 (1992).
6. REST, J., "Modeling the Behavior of Xe, I, Cs, Te, Ba and Sr in Solid and Liquefied Fuel During Severe Accidents", J. Nucl. Mater., **150**, 203 (1987).
7. BRITO, A.C., IGLESIAS, F.C., LIU, Y., PETRILLI, M.A., RICHARDS, M.J., CRIBB, R.A. and REID, P.J., "SOURCE 2.0: A Computer Program to Calculate Fission Product Release from Multiple Fuel Elements for Reactor Scenarios," Fourth International Conference on CANDU Fuel in Pembroke, Ontario, 1-4 Oct (1995).
8. OSBORNE, M.F. and LORENZ, R.A., "ORNL Studies of Fission Product Release Under LWR Severe Accident Conditions", Nuclear Safety, **33**, No. 3, 334 (1992)
9. LEWIS, B.J., ANDRE, B., MOREL, B., DEHAUDT, P., MARO, D., PURDY, P.L., COX, D.S., IGLESIAS, F.C., OSBORNE, M.F. and LORENZ, R.A., "Modelling the Release Behaviour of Cesium During Severe Fuel Degradation", J. Nucl. Mater., **227**, 83 (1995).
10. RUMMELHART, D.E. and MCLELLAND, J.L., "Parallel Distributed Processing: Explorations in the Microstructure of Cognition Volume 1: Foundations", MIT Press, Cambridge (1986).
11. NEURALWARE, "Reference Guide for NeuralWorks Professional II/PLUS and NeuralWorks Explorer", Pittsburgh, PA (1991).
12. MASON, R.L., GUNST, R.F. and J.L. Hess, "Statistical Design and Analysis of Experiments with Applications to Engineering and Science", John Wiley & Sons, New York (1989).
13. LEWIS, B.J., COX, D.S. and IGLESIAS, F.C., "A Kinetic Model for Fission-Product Release and Fuel Oxidation Behaviour for Zircaloy-Clad Fuel Elements Under Reactor Accident Conditions", J. Nucl. Mater., **207**, 228 (1993).
14. HARNDEN-GILLIS, A.C., LEWIS, B.J., ANDREWS, W.S., PURDY, P.L., OSBORNE, M.F. and LORENZ, R.A., "Modelling of Cesium Release from Light Water Reactor Fuel Under Severe Accident Conditions", Nucl. Technol., **109**, 39 (1995).
15. ANDREWS, W.S., "Modelling the Release of Volatile Fission Products from Nuclear Reactor Fuel Under Severe Accident Conditions Using Artificial Neural Networks", Doctor of Philosophy (Nuclear Engineering) Dissertation, Department of Chemistry and Chemical Engineering, Royal Military College (1995).

TABLE 1. VARIABLES AND PARAMETERS USED IN INPUT SPACE FOR DEVELOPING ANN, INCLUDING MAXIMUM AND MINIMUM VALUES. NODES ARE DEPICTED IN FIGURE 1.

Node Number (i)	Variable (v _i)	Minimum Value (m _i)	Maximum Value (M _i)
0	Bias (value fixed at 1)		
1	Time above 1000°C (s)	-3320	22507
2	Fuel Temperature (°C)	435	2090
3	Time at Temperature (s)	0	22195
4	Time in Steam (s)	0	10892
5	Time in Air (s)	0	11490
6	Rate of Temperature Change (°C/s)	-0.2	0.5
7	Weight of Zircaloy (g)	0	8.9
8	Cladding closed (y or n)	0	1
9	Rate of Steam Flow (mL/min)	0	200
10	Rate of Air Flow (mL/min)	0	400
11	Rate of Inert Gas Flow (mL/min)	0	800
12	Peak Linear Power (kW/m)	43	58
13	Burnup (MWh/kgU)	257	570
14	Weight of Fuel (g)	.191	45.761

TABLE 2. STATISTICAL ATTRIBUTES OF MODELS APPLIED TO VALIDATION SET (HCE2-CM6). MODELS ARE DEPICTED GRAPHICALLY IN FIGURES 5 AND 6.

Model	Correlation Coefficient r	Normalized Error E _n	Average Absolute Error E _{abs}
ANN	0.995	0.064	0.054
Lewis (steam)	0.992	0.056	0.038
CORSOR-M	0.979	1.523	0.270

TABLE 3. RANKING OF RELATIVE IMPORTANCE OF INPUT VARIABLES BASED ON SENSITIVITY AND WEIGHT SPACE ANALYSIS

VARIABLE
Temperature
Time Sample above 1000°C
Time in Air
Time at Temperature
Time in Steam
Zircaloy Weight
Steam Flow Rate
Cladding open
Fuel weight
Linear power
Burnup
Temperature change rate
Air flow rate
Inert gas flow rate

TABLE 4. CONNECTION WEIGHTS w_{ji} AND w_{kj} FOR A 14-5-1 TRAINED ANN

Source Node	Destination Node					
	15	16	17	18	19	20
0	-0.4305	0.2578	0.0018	0.0606	-0.1546	0.4668
1	-1.5001	0.8345	-0.6655	-1.2945	-0.1987	
2	0.0521	-2.0045	-1.0748	-2.2791	-0.9801	
3	-0.2716	-0.5367	-0.0451	0.2944	0.09358	
4	-0.5602	-0.6749	-0.2416	-1.9599	-0.0978	
5	-1.8507	0.1387	-0.4572	-0.0618	-0.0943	
6	1.1470	-0.4846	1.1114	2.5243	0.5328	
7	1.2937	-0.4971	0.1895	0.7858	0.2406	
8	-0.6041	0.4703	-0.0633	-0.4438	0.3048	
9	-0.3888	0.4718	-0.1081	-0.7703	-0.0689	
10	-0.8062	-0.0842	0.1111	0.4438	-0.1239	
11	0.6468	-0.1865	-0.0033	0.2545	-0.0193	
12	-0.9383	-0.8495	-0.6413	-0.5259	-0.1234	
13	0.8866	1.0589	0.5407	1.1923	0.3248	
14	0.4028	-0.2117	-0.1219	-0.2636	-0.0983	
15						-0.5391
16						-0.4932
17						-0.0579
18						-0.3824
19						0.2102

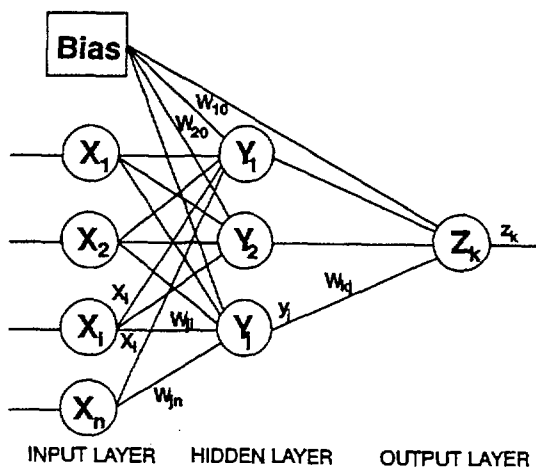


FIGURE 1. ARCHITECTURE OF A BACK PROPAGATION ARTIFICIAL NEURAL NETWORK. DESCRIPTION OF INPUT VARIABLES IN TABLE 1 AND CONNECTION WEIGHTS IN TABLE 4.

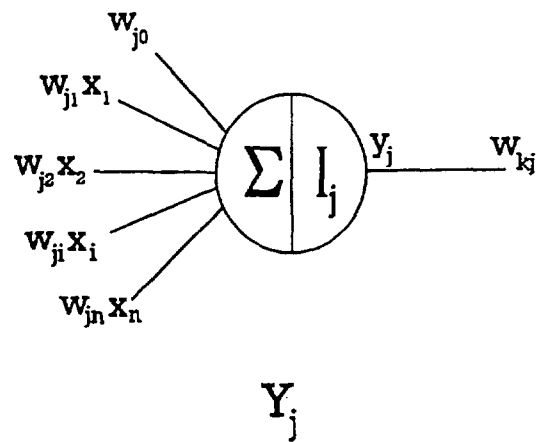


FIGURE 2. ARCHITECTURE OF J^{th} NEURON IN THE HIDDEN LAYER

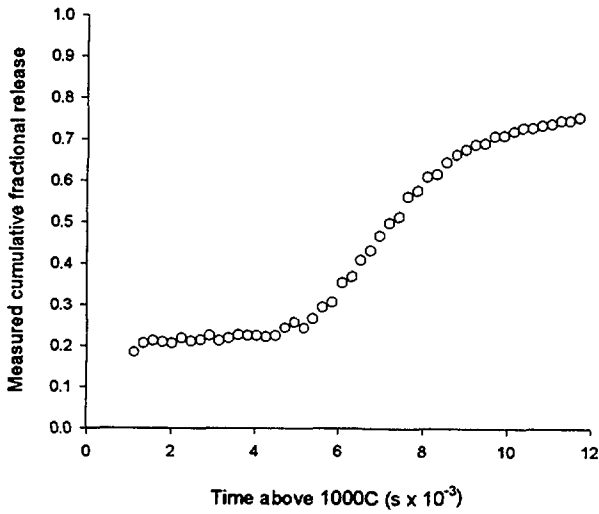


FIGURE 3. TYPICAL DATA DISTRIBUTION FOR CRL TEST (HCE2-CM2).

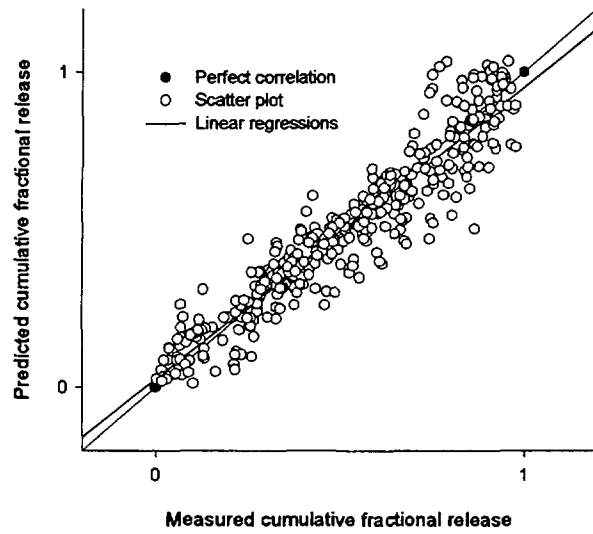


FIGURE 4. SCATTER PLOT OF 386 DATA POINT TEST SET OF 14-5-1 ANN MODEL.

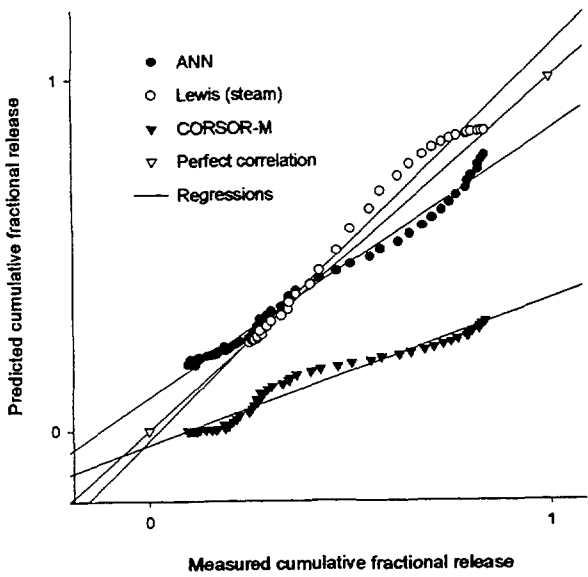


FIGURE 5. SCATTER PLOTS OF MODELS PREDICTING CUMULATIVE FRACTIONAL RELEASE FOR VALIDATION SET (HCE2-CM6). STATISTICAL COMPARISON IN TABLE 2.

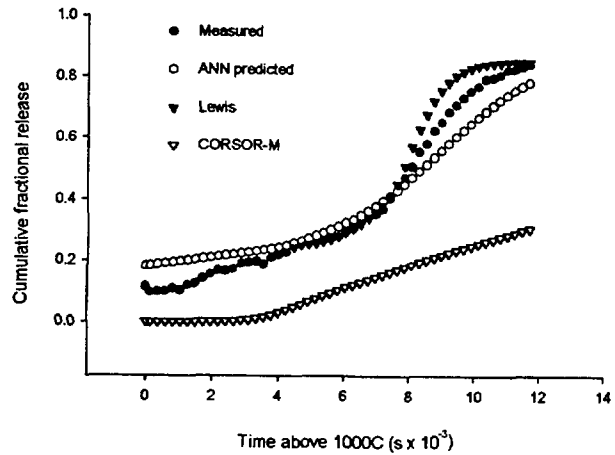


FIGURE 6. COMPARISON OF MODEL PERFORMANCE PREDICTING FRACTIONAL RELEASE FOR VALIDATION SET (HCE2-CM6). STATISTICAL COMPARISON IN TABLE 2.